Imaging Agents

DOI: 10.1002/anie.200604738

Hybrid Silica Nanoparticles for Multimodal Imaging**

*William J. Rieter, Jason S. Kim, Kathryn M. L. Taylor, Hongyu An, Weili Lin, Teresa Tarrant, and Wenbin Lin**

Recent applications of luminescent nanoparticles in biological and biomedical imaging[1] underscore the need for developing novel nanomaterials for use in other imaging modalities.[2] Among them, magnetic resonance imaging (MRI) has emerged as the most powerful diagnostic tool owing to its noninvasive nature, intrinsically high spatial resolution, and reliance on nonradioactive contrast agents.[3] Although many MRI contrast agents are currently available for clinical use, the vast majority of them (with the exception of iron oxide nanoparticles) are gadolinium- or manganese-based coordination complexes that need to be administered in high concentrations to provide satisfactory image contrast enhancements.[3] With the ability to carry large payloads of active magnetic centers,[4] nanoparticulate MR contrast agents can work at much lower concentrations and thus be made target-specific by labeling desired cells through phagocytic pathways or by conjugation to affinity molecules specific to cell surface markers.

Pioneering work by Weissleder et al. and others has demonstrated the utility of iron oxide nanoparticles as target-specific MR contrast agents for tumor angiogenesis, inflammation, and gene expression.[5] Owing to the enhanced transverse relaxation of water protons, iron oxide nanoparticles are typically used in *T*2-weighted MRI, which leads to the reduction of signal intensity. It is desirable to have new nanomaterials that enhance signal intensities in *T*1-weighted MRI. Gd^{3+}-containing microemulsions elegantly developed by Lanza, Wickline, and Morawski have provided an interesting platform for designing nanoscale *T*1 contrast agents.[6] Further development of nanoscale MR contrast agents will, however, require new nanomaterials that are able to carry high payloads of magnetic centers. Herein, we report our design of robust luminescent and paramagnetic hybrid silica nanoparticles with very high payloads of magnetic centers and their use as multimodal contrast agents for in vitro optical and *T*1- and *T*2-weighted MR imaging. We demonstrate efficient uptake of these nanoparticles by monocyte cells, which may provide a mechanism for target-specific MRI of inflammations by selective trafficking of labeled monocyte cells.

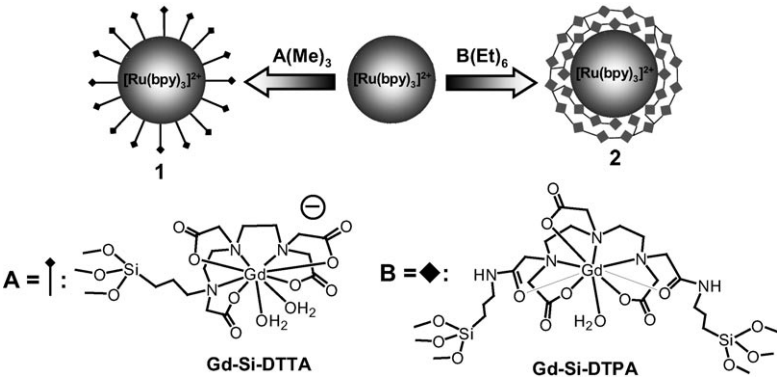

Scheme 1. Synthesis of hybrid silica nanoparticles **1** and **2**.

Hybrid silica nanoparticles **1** containing a luminescent $[Ru(bpy)_3]Cl_2$ core (bpy = 2,2′-bypyridine) and a paramagnetic monolayer coating of a silylated Gd complex were prepared by a well-established water-in-oil reverse microemulsion synthetic procedure (Scheme 1).[7] Specifically, nanoparticles of **1** were prepared by adding ammonia (0.8 mL) to a clear microemulsion of water (2.28 mL), $[Ru(bpy)_3]Cl_2$ (0.16 mL, 0.1 M solution in water), and tetraethoxysilane (TEOS, 0.4 mL) in a Triton X-100 (0.3 M)/1-hexanol (1.5 M)/cyclohexane solution (40 mL) to initiate the hydrolysis process. After stirring at room temperature for approximately 24 h, gadolinium (trimethoxysilylpropyl)diethylenetriaminetetraacetate solution (Gd-Si-DTTA; 1.0 mL, 0.12 M in water) was added and the reaction mixture was stirred for an additional 24 h. Nanoparticles of **1** (ca. 150 mg) were isolated by centrifugation after the addition of an equal volume of methanol and subsequent washing with methanol and water. Scanning electron microscopy (SEM) and trans-

[*] W. J. Rieter, J. S. Kim, K. M. L. Taylor, Prof. W. Lin
Department of Chemistry, CB#3290
University of North Carolina
Chapel Hill, NC 27599 (USA)
Fax: (+1) 919-962-2388
E-mail: wlin@unc.edu
Homepage:
http://www.chem.unc.edu/people/faculty/linw/wlindex.html
Dr. H. An, Prof. W. Lin
Department of Radiology
University of North Carolina
Chapel Hill, NC 27599 (USA)
Prof. T. Tarrant
Thurston Arthritis Research Center and
Department of Medicine
University of North Carolina
Chapel Hill, NC 27599 (USA)

[**] We acknowledge financial support from NIH (U54-CA119343 and P20 RR020764). We thank Ms. Kathy Wilber for experimental help. W.J.R. thanks NSF for a graduate fellowship and W.L. is a Camille Dreyfus Teacher–Scholar.

Supporting information for this article is available on the WWW under http://www.angewandte.org or from the author.

mission electron microscopy (TEM) images indicated that nanoparticles of **1** from the above synthesis ($W = 15$, where W is the molar ratio of water to surfactant) exhibit a monodisperse spherical morphology with a diameter of approximately 37 nm (Figure 1). This synthesis is highly reproducible

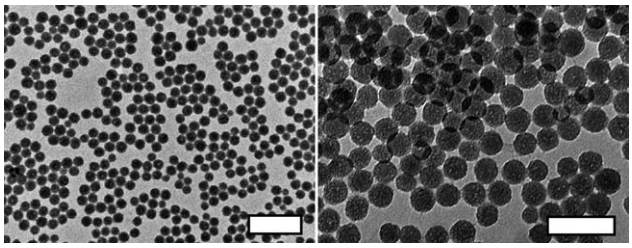

Figure 1. TEM images of nanoparticles of **1** (left) and **2** (right) synthesized with a W value of 15. The scale bars represent 200 (left) and 100 nm (right), respectively.

and the nanoparticle diameters are controllable by the W values of the microemlusions. Nanoparticles of **1** with an average diameter of 37 nm were used for subsequent studies. The Si-DTTA ligand used provides seven binding sites for Gd^{3+} ions, so that the toxicity of the nanoparticles (owing to leaching of Gd^{3+} centers) can be minimized.

Thermogravimetric analysis (TGA) of **1** showed an initial weight loss of 12% from room temperature to 180°C and a further weight loss of 11% from 180 to 450°C, which correspond to the adsorbed solvent species and the organic components of Gd-DTTA, respectively. Direct current plasma (DCP) measurements indicated that **1** contained approximately 4.3 wt% Gd. The TGA and DCP results correspond to a loading of about 10200 Gd-DTTA/particle. A dispersion of **1** in water showed a ligand-to-metal charge transfer (LMCT) absorption peak around 450 nm and an emission peak at 595 nm ($\lambda_{ex} = 488$ nm) for the incorporated $[Ru(bpy)_3]Cl_2$. We have determined the MR relaxivities of **1** using a 3.0-T full-body MR scanner. Nanoparticles of **1** have a longitudinal relaxivity ($r1$) of 19.7 s^{-1} and a transverse relaxivity ($r2$) of 60.0 s^{-1} on a per millimolar Gd^{3+}-ion basis (Figure 2). These relaxivity values are much higher than those of the Gd-Si-DTTA complex ($r1 = 6.8$ and $r2 = 7.0$ s^{-1} mM^{-1} Gd^{3+} ions), presumably as a result of the reduced tumbling rates of **1** in aqueous solution. Because of the high payload of Gd-DTTA chelates, nanoparticles of **1** display $r1$ and $r2$ values of 2.0×10^5 and 6.1×10^5 s^{-1}, respectively, on a per millimolar particles basis.

We have also attempted to increase Gd^{3+}-ion loading by using a bis(silylated)-Gd-DTPA (DTPA = diethylenetriaminepentaacetate) complex (Gd-Si-DTPA) in the microemulsion reaction (Scheme 1). Nanoparticles of **2** were obtained from the same procedures applied for **1,** and were characterized using SEM, TEM, TGA, DCP, and relaxivity measurements. Nanoparticles of **2** have an average diameter of 40 nm (Figure 1). TGA and DCP results (see the Supporting Information) indicate that **2** has a loading of approximately 63200 Gd-DTPA/particle, which suggests that unlike Gd-Si-DTTA in **1**, the Gd-Si-DTPA chelates in **2** can form multilayers on the silica nanoparticle to lead to a thick coating of

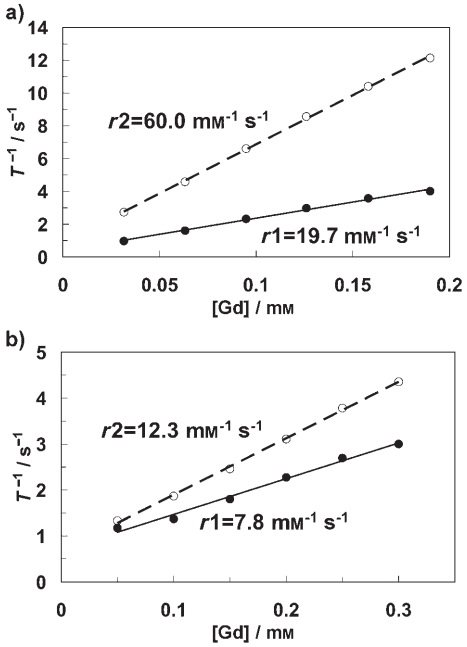

Figure 2. a) $r1$ and $r2$ relaxivity curves of **1** (diameter ca. 37 nm). b) $r1$ and $r2$ relaxivity curves of **2** (diameter ca. 40 nm).

siloxane polymer. Relaxivity measurements, however, indicate that for **2**, $r1 = 7.8$ and $r2 = 12.3$ s^{-1} on a per millimolar Gd^{3+}-ion basis. For comparison, the Gd-Si-DTPA complex has an $r1$ and $r2$ of 6.2 and 8.0 s^{-1} per millimolar Gd^{3+} ions, respectively. The relaxivity values exhibited by **2** are much lower than those of **1**, presumably because the Gd^{3+} centers in the inner layers are not readily accessible to water molecules. Nonetheless, **2** still has an impressive $r1 = 4.9 \times 10^5$ and $r2 = 7.8 \times 10^5$ s^{-1} per millimolar particles, respectively.

Given their high relaxivities and stabilities, we have tested the efficacy of nanoparticles of **1** as multimodal in vitro imaging contrast agents. An immortalized monocyte cell line was used for this study because of its phagocytic capacity as well as its important role in autoimmune diseases, such as rheumatoid arthritis.[8] Laser scanning confocal fluorescence microscopic studies clearly indicated the efficient uptake of **1** by monocyte cells after they were incubated with 2 mL of medium containing 0.42 mg of **1** for 0.5 h. The LMCT luminescence of $[Ru(bpy)_3]Cl_2$ is clearly visible in the confocal z-section images (Figures 3a and b). Quantification with flow cytometric measurements indicated that monocyte labeling efficiency with **1** is greater than 98% (Figure 3e). More importantly, we have successfully observed MR image enhancements of the labeled monocytes when compared with a control of unlabeled monocytes. To prepare the cells for MRI, we incubated approximately 18×10^6 cells in 1.4 mL of media containing 10.65 mg of **1** for 1 h. The cells were isolated by centrifuge, washed twice with phosphate-buffered saline (PBS) solution, pelleted, and covered with 200 μL of a PBS buffer layer. As shown circled in Figures 3c and d, significant positive signal enhancement in the $T1$-weighted image and negative signal enhancement in the $T2$-weighted image were observed for the labeled cells, depending on the MR pulse sequence employed. Finally, 3-(4,5-dimethylthiazol-2-yl)-5-

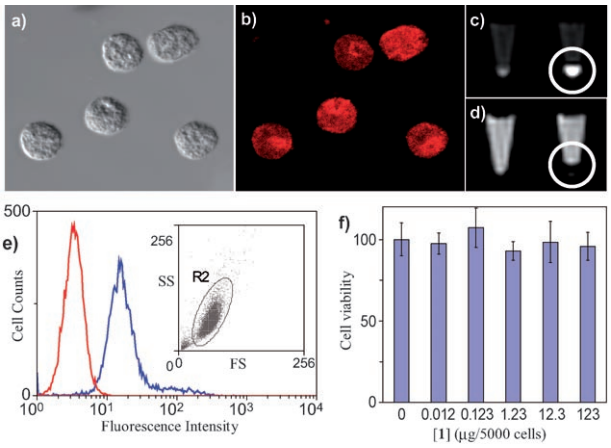

Figure 3. Microscopic images of **1**-labeled monocyte cells: a) optical; b) laser scanning confocal fluorescence. c),d) MR images of unlabeled (left) and **1**-labeled (right) monocyte cells: c) *T*1-weighted and d) *T*2-weighted. e) Flow cytometric results for the unlabeled (red) and **1**-labeled (blue) monocyte cells indicating greater than 98% labeling efficiency (the inset shows the purity of the labeled cells; SS = side scatter, FS = forward scatter). f) MTS assay of the monocyte cells incubated with different amounts of **1**.

(3-carboxymethoxyphenyl)-2-(4-sulfophenyl)-2*H*-tetrazolium (MTS) cell-viability assays showed that nanoparticles of **1** were not toxic to monocyte cells; they were completely viable even after incubation with a nanoparticle loading as high as 0.123 mg per 5000 monocyte cells.

In summary, we have designed robust hybrid silica nanoparticles containing a luminescent core and a paramagnetic coating. Their utility as optical and MR imaging contrast agents has been clearly demonstrated. Monocyte cells have been efficiently labeled with these hybrid particles to allow their multimodal in vitro imaging. We are currently evaluating the efficacy of these hybrid nanomaterials as target-specific contrast agents for optical and MR imaging of rheumatoid arthritis in mice.

Experimental Section

A typical synthesis of **2**: $[Ru(bpy)_3]^{2+}$-doped hybrid silica nanoparticles with the Gd-Si-DTPA coating were prepared by adding distilled H_2O, a $[Ru(bpy)_3]^{2+}$ aqueous solution (0.1 M), and TEOS to a 0.3 M Triton X-100/1.5 M 1-hexanol/cyclohexane stock solution that was stirred vigorously at room temperature. After 10 min of vigorous stirring, aqueous NH_4OH was added to initiate hydrolysis, and the resultant optically transparent red microemulsion mixture was stirred for another 24 h at room temperature. A gadolinium bis(aminopropyltriethoxysilyl)diethylenetriaminepentaacetate (Gd-Si-DTPA) solution (0.2 M) was then added to the mixture, which was stirred for an additional 12 h. The Gd-Si-DTPA functionalized silica nanoparticles were then precipitated with an equivalent volume of methanol and isolated by centrifuge at 12500 rpm for 30 min. The nanoparticles were subsequently washed twice with MeOH by redispersing by sonication and twice with H_2O before redispersing them in water. Further details are given in the main text.

Confocal imaging of labeled monocyte cells: Monocyte cells were incubated in media (2.0 mL) with nanoparticle suspension (17.0 μL, 24.6 mg mL^{-1}) for 30 min at 37 °C with 5% CO_2. The cells were isolated from the media by centrifugation at 1000 RPM for 10 min at 4 °C, and subsequently washed with a fresh aliquot of media. The resulting isolated pellet was suspended in 100 μL of PBS and imaged using confocal microscopy: excitation at 488 nm, emission using 530 LP filter settings, and 252 × zoom (63 × oil-immersion optical, 4 × digital).

MTS cell-viability assay: Monocyte cells were counted by trypan blue exclusion and distributed into a 96-well plate at a concentration of 5000 cells in 100 μL per well. Cells were incubated with various concentrations of **1**: 123, 12.3, 1.23, 0.123, 0.0123, and 0 μg in 5 μL of distilled H_2O. After 20 h of incubation, MTS solution (20 μL) was added to each well and allowed to further incubate for 4 h. The microplate was read for 492 nm absorbance at $t = 0$ and $t = 4$ h after MTS addition. The changes in absorbance (from $t = 0 \rightarrow 4$ h) were necessary to subtract nanoparticle background from the viability assay.

Received: November 21, 2006
Published online: April 5, 2007

Keywords: gadolinium · imaging agents · magnetic resonance imaging · nanostructures · silicon

[1] a) A. P. Alivisatos, *Nat. Biotechnol.* **2004**, *22*, 47; b) S.-W. Kim, J. P. Zimmer, S. Ohnishi, J. B. Tracy, J. V. Frangioni, M. G. Bawendi, *J. Am. Chem. Soc.* **2005**, *127*, 10526; c) X. Gao, Y. Cui, R. M. Levenson, L. W. K. Chung, S. Nie, *Nat. Biotechnol.* **2004**, *22*, 969; d) B. N. G. Giepmans, S. R. Adams, M. H. Ellisman, R. Y. Tsien, *Science* **2006**, *312*, 217; e) M. G. Sandros, D. Gao, D. E. Benson, *J. Am. Chem. Soc.* **2005**, *127*, 12198 – 12199.

[2] M. M.-C. Cheng, G. Cuda, Y. L. Bunimovich, M. Gaspari, J. R. Heath, H. D. Hill, C. A. Mirkin, A. J. Nijdam, R. Terracciano, T. Thundat, M. Ferrari, *Curr. Opin. Chem. Biol.* **2006**, *10*, 11.

[3] a) É. Toth, L. Helm, A. E. Merbach, *The Chemistry of Contrast Agents in Medical Magnetic Resonance Imaging*, Wiley, Chichester, **2001**; b) P. Caravan, J. J. Ellison, T. J. McMurry, R. B. Lauffer, *Chem. Rev.* **1999**, *99*, 2293; c) K. N. Raymond, V. C. Pierre, *Bioconjugate Chem.* **2005**, *16*, 3.

[4] W. S. Seo, J. H. Lee, X. Sun, Y. Suzuki, D. Mann, Z. Liu, M. Terashima, P. C. Yang, M. V. McConnell, D. G. Nishimura, H. Dai, *Nat. Mater.* **2006**, *5*, 971.

[5] a) R. Weissleder, A. Moore, U. Mahmood, R. Bhorade, H. Benveniste, E. A. Chiocca, J. P. Basilion, *Nat. Med.* **2000**, *6*, 351; b) H.-T. Song, J.-S. Choi, Y.-M. Huh, S. Kim, Y.-W. Jun, J.-S. Suh, J. Cheon, *J. Am. Chem. Soc.* **2005**, *127*, 9992 – 9993.

[6] A. M. Morawski, G. A. Lanza, S. A. Wickline, *Curr. Opin. Biotechnol.* **2005**, *16*, 89.

[7] a) U. Jeong, Y. Wang, M. Ibisate, Y. Xia, *Adv. Funct. Mater.* **2005**, *15*, 1907; b) L. Wang, W. Tan, *Nano Lett.* **2006**, *6*, 84; c) G. Yao, L. Wang, Y. Wu, J. Smith, J. Xu, W. Zhao, E. Lee, W. Tan, *Anal. Bioanal. Chem.* **2006**, *385*, 518 – 524; d) S. Santra, R. P. Bagwe, D. Dutta, J. T. Stanley, G. A. Walter, W. Tan, B. M. Moudgil, R. A. Mericle, *Adv. Mater.* **2005**, *17*, 2165 – 2169; e) I. Roy, T. Y. Ohulchanskyy, D. J. Bharali, H. E. Pudavar, R. A. Mistretta, N. Kaur, P. N. Prasad, *Proc. Natl. Acad. Sci. USA* **2005**, *102*, 279 – 284; f) D. R. Radu, C.-Y. Lai, K. Jeftinija, E. W. Rowe, S. Jeftinija, V. S.-Y. Lin, *J. Am. Chem. Soc.* **2004**, *126*, 13216.

[8] Y. Ma, R. M. Pope, *Curr. Pharm. Des.* **2005**, *11*, 569.

